Electrical conductivity of tungsten near its critical point

A. Kloss, T. Motzke, R. Grossjohann, and H. Hess

Institute of Low-Temperature Plasma Physics at the Ernst-Moritz-Arndt-University Greifswald,
Robert-Blum-Strasse 8-10, D-17489 Greifswald, Germany

Electrical conductivity of fluid tungsten under subcritical and supercritical conditions has been measured. Fast wire explosions are used to create the corresponding states. The heavy-particle density varies from 4×10^{21} to 6×10^{22} cm^{-3}, the temperature from 3700 up to 13 000 K. The measured electrical conductivity mainly depends on the averaged density and seems to be independent of the temperature within the experimental errors. The measurements are compared with theoretical models. [S1063-651X(96)14011-3]

PACS number(s): 52.80.−s, 72.15.Cz, 05.70.Jk

I. INTRODUCTION

The electrical conductivity in expanded alkali metals under subcritical and supercritical conditions around the critical point is well established by experimental as well as by theoretical investigations [1–4]. Much less information is available about other metals in the corresponding state. In some recently published papers the attempt has been made to study the transport properties of different expanded fluid metals in dependence upon the so-called nonideality or coupling parameter Γ [5–8]. This parameter is defined as the ratio of the potential energy of the particles to their kinetic energy. In the mentioned papers the parameter is only given for ions,

$$\Gamma = \frac{z^2 e^2}{akT} \approx 2.69\times10^{-3}\ \frac{z^2 n_i^{1/3}}{T}\ \text{cm K}, \qquad (1)$$

where $a=(3/4\pi n_i)^{1/3}$ is the ion sphere radius, n_i the ion density, and z the average ionization level. Plasmas are nonideal or strongly coupled for $\Gamma \gtrsim 1$. If the Fermi energy becomes higher than the thermal energy of the fluid, the electron component will be degenerate; the degeneracy parameter Θ is given by

$$\Theta \approx \frac{h^2 n_e^{2/3}}{8m_e kT} \approx 4.37\times10^{-11}\ \frac{n_e^{2/3}}{T}\ \text{cm}^2\ \text{K}; \qquad (2)$$

$\Theta \gg 1$ means complete degeneracy of the electrons.

The plasma produced by Benage *et al.* [6] (capillary discharges) shows intermediate coupling ($\Gamma < 1$) and is clearly nondegenerate [$\Theta \ll 1$ due to the high temperature (25 eV) and the low density (5×10^{21} cm^{-3})]. The plasmas investigated by Shepherd, Kania, and Jones [5] (capillary discharges) and by DeSilva and Kunze [7,8] (wire explosions in capillaries or water) are more strongly coupled ($\Gamma \gtrsim 1$) and at least partially degenerate ($\Theta \gtrsim 1$).

In this paper, measurements of the electrical conductivity in strongly coupled *and* degenerate plasmas ($\Gamma \gg 1, \Theta > 1$) similar to [9] are presented. The plasmas have been produced by rapid heating of a wire-shaped probe of the studied metal (tungsten) using a fast electrical discharge (wire explosion). Typical parameters of our experiments are temperatures between 3700 and 13 000 K and ion densities between 4×10^{21} and 6×10^{22} cm^{-3}. The number of free electrons per atom z near the solid-state density should be about 6 [10]. Near the critical point—at the lowest density a liquid can have—this number should be about 3 [11].

II. EXPERIMENTAL SETUP AND MEASUREMENTS

As shown in Fig. 1, a capacitor 1 (675 nF) is discharged through a tungsten wire 4 (diameter 100 μm, length 5 mm) in a low-inductance ($\sim$53 nH including the wire) coaxial circuit. The discharge is switched with a spark gap 2 which is optically triggered by a second small ignition spark 9. The ground conductor 7 encapsulates the whole discharge coaxially. This also suppresses electromagnetic disturbances of the measurements.

In order to obtain the conductivity of the wire, it is necessary to measure the current through it, the voltage across it, and its diameter, and to make some assumptions about the nature of the process observed. Further a temperature is determined to have some indications of the thermodynamic state of the expanding metal.

The current measurement is carried out simultaneously in two ways, measuring the voltage over a known coaxial shunt resistor 5 and integrating a dI/dt signal (I denotes current) of a Rogowski coil [12] that surrounds the wire holder 3b. Both signals are in sufficiently good agreement, but the integral signal is more precise for the faster first part of the discharge whereas the shunt signal measured with higher gain level gives more accuracy for the later time.

The voltage is measured between the wire holders 3a and 3b with a compensated high voltage probe (Tektronix P6015A) and is simultaneously recorded by two channels
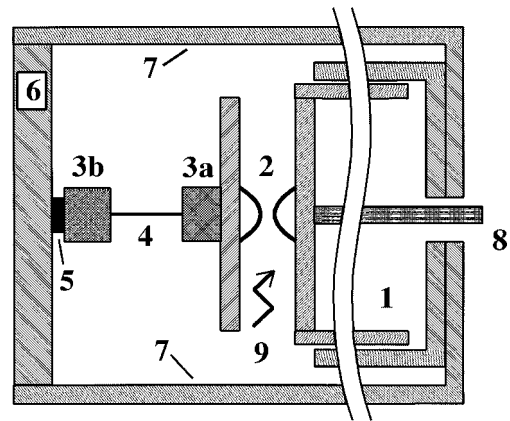

FIG. 1. Scheme of the discharge chamber. 1, tube capacitor; 2, spark gap; 3a and b, wire holder; 4, wire; 5, shunt resistor; 6, Cu ground plate; 7, ground conductor; 8, HV supply; 9, ignition spark.
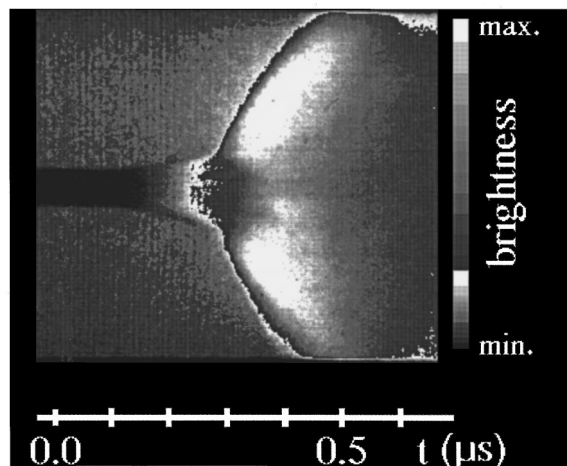
FIG. 2. Streak image with backlighting: $E_{max} = 650$ kJ/mol.

FIG. 3. Voltage U, current I, resistance R, dissipated energy E, radius r, temperature T (surface, —, bulk (calculated), $\cdots$); $E_{max} = 650$ kJ/mol.

with different gain levels. The inductive part of the measured voltage is subtracted using the dI/dt signal from the Rogowski coil and taking into account the inductances of the wire and the inductance of the measuring circuit. The error of voltage due to the changing of the inductances during the discharge can be assumed to be less than 1%. All electrical measurements are carried out with an accuracy of 1%.

The radius of the expanding wire is obtained from streak images (Fig. 2). These images are made at a wavelength $\lambda = (650 \pm 40)$ nm with the slit of the camera perpendicular to the wire axis. They show the radial distribution of brightness versus time. The (local) differences of the maximal first derivatives of the distribution of brightness are calculated for every time and taken to be the diameter of the expanding wire. For the early time, when the wire is still cold, backlighting is used. For the later time, the self-emitting area is taken. In that way the diameter is determined with an error of $\pm 5\%$. Until the end of melting, the volume expansion data from [13] support our results.

In addition, the following usual [5–9] but not necessarily correct assumptions are made. The whole material of the wire is contained and homogeneously distributed within the determined diameter. The temperature is distributed homogeneously as well. Later investigations and a more complex dynamic model that is in progress should give a more precise idea of this process.

From the diameter, cross section, and density of the wire material, and using the Ohmic voltage and the current measured, the conductivity has been calculated. The measuring error is calculated from the different data mentioned above and indicated in Fig. 5 on the measured curve.

A temperature of the wire is determined in two ways. The surface temperature is calculated from the brightness signal of a 15-μm spot on the surface of the wire at $\lambda = (650 \pm 40)$ nm. This signal shows an obvious plateau at the melting of the wire. The length of this plateau corresponds to the melting energy. The melting temperature is well known and constant up to a pressure of many kbars. Assuming emissivity of the liquid to be constant for all temperatures above the melting and equal that at the melting point—as is often done because of the lack of relevant data—the surface temperature is obtained by Planck's law (the radiation comes out from a sheath with an optical depth
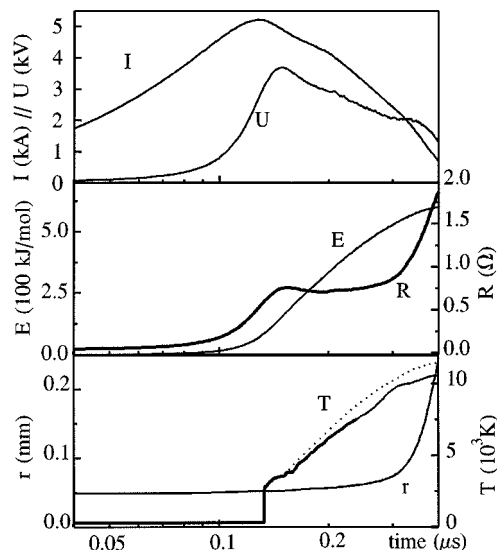
equal to 1). For this procedure the knowledge of the absolute value of the emissivity is not necessary. A deviation of the emissivity of 20% from this constancy would cause a rising error of the calculated temperature from 3.3% to 9.1% in the temperature range from 4000 to 12 000 K.

A second temperature estimation may be obtained from the electric energy dissipated in the wire material and an assumption about a relevant specific heat. The pressure during the discharge is caused by fast heating of the material and by the inhibition of the corresponding expansion due to the inertia of the particles and the magnetic field of the discharge current (pinch effect). The ''dynamic'' as well as the ''magnetic'' pressure can be estimated—from the acceleration of the wire edge for the one and from its radius and the electric current for the other—both in a reasonable order of magnitude of about some kbars depending on the rate of current rising. From the melting up to the onset of vaporization, the pressure approximately remains constant.

This allows a temperature estimation—now for a bulk temperature—assuming a quasi-isobaric process and using therefore a specific heat at constant pressure c_p which is given by different authors within $\pm 10\%$ and assumed to be constant in the expanding liquid [14]. Being aware of the very complex topology of the specific heats at both sides of the coexistence line (in a p-T diagram) and especially around the critical point, we nevertheless consider it as a reasonable zero approximation to calculate the bulk temperature just with this specific heat due to the lack of information about the other quantities.

Generally, the calculation should go along these lines: With the onset of vaporization, the corresponding latent heat has to be taken into account (the higher the pressure, the lower the heat, which tends to zero approaching the critical point). Assuming thermodynamic equilibrium (the vaporization immediately follows the energy input; the relaxation time of vaporization is small compared with the time resolution in experiment), the temperature during the vaporization should be constant. Depending upon the available energy,
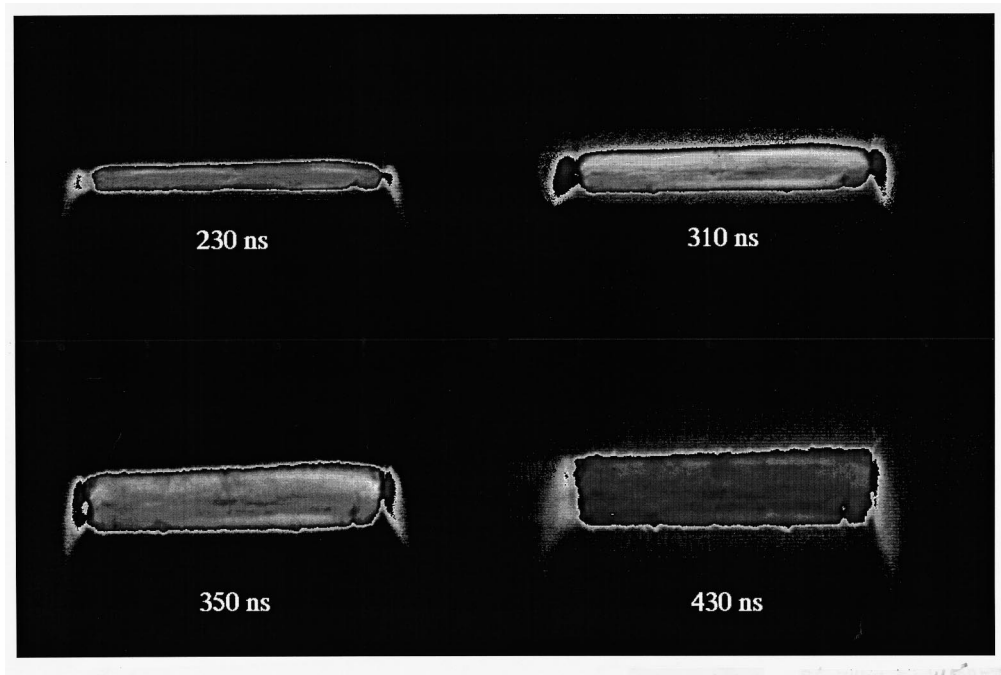
FIG. 4. Framing images of a wire explosion at 230, 310, 350, and 430 ns with an exposure time of 10 ns; $E_{max} = 650$ kJ/mol.

the wire material may arrive in the gaseous state. Now the process will be neither isobaric nor isochoric; the corresponding specific heat should then be smaller than in the liquid (anywhere between $3R/2$ and $5R/2$—the ideal-gas values).

The radiated power at 10 000 K according to the Stefan-Boltzmann law is below 0.1% of the dissipated power and can therefore be neglected. The voltage of the capacitor ranged from 2.3 to 5.5 kV. This corresponds to a maximal dissipated energy E_{max} in the wire material from 350 to 2000 kJ/mol. A value of 1200 kJ/mol should be sufficient for total evaporation [15]. A further increase of the discharge voltage would cause discharges beside the wire or along its surface which would interfere with the electrical and optical measurements.

A set of measured data from a shot with an energy input E_{max} of 650 kJ/mol is plotted in Fig. 3 over a logarithmic time scale. After 300 ns the onset of the strong expansion due to evaporation and the increase of resistance can be seen.

The framing images in Fig. 4 taken from the same shot with an exposure time $\Delta t = 10$ ns show the homogeneity of the process. They also prove that there is no length expansion which would cause a slipping to the side. The cylindrical shape remains well preserved. This stable behavior was also observed at larger Ni tubes in [16] up to a discharge time of 80 μs.

The experiments are carried out with ''technical'' tungsten wire from NARVA [17] as it is used in the light-bulb production with a diameter of 100 μm. It was manufactured by powder metallurgy. Its cold resistance (7.87 Ω/m) is higher compared with that of Goodfellow wire (6.87 Ω/m). The wire has a black color due to an oxide layer of about 0.1 μm. This may be the reason for the good inhibition of surface discharges. The work function of tungsten oxide is 6.24 eV while it is 4.53 eV for pure tungsten [18]. This causes a thermal emission of electrons that is two to three orders of

magnitude lower for tungsten oxide due to the Richardson equation. Using ''clean'' Goodfellow wire or cleaned NARVA wire even at lower discharge voltages very intensive surface discharges can be observed as they were reported in [19].
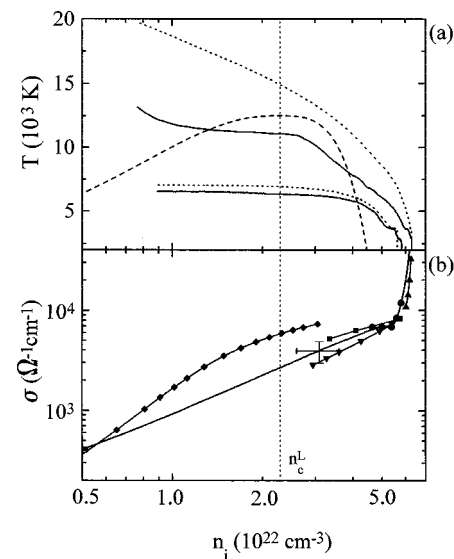

FIG. 5. (a) Bulk temperature ($\cdots$) and measured temperature (—) of the wire versus heavy particle density for wire explosions with highest (upper curves, $E_{max} = 2000$ kJ/mol) and lowest (lower curves, $E_{max} = 350$ kJ/mol) energy input; two phase region (- - -) [20]. (b) Averaged measured conductivity of tungsten (—) versus heavy particle density; other experimental results from Hixson and Winkler [13] (2650–5690 K) (–●–), Zwikker [21] (1200–3400 K) (–▲–), Seydel, Fucke, and Wadle [22] (3680–7500 K) (–■–), theoretical calculations according to Ziman ($z = 6$) [23] (–▼–), and Likalter ($z = 3$), $T = 12\,500$ K) [24] (–◆–); n_c^L critical density according to [11].

III. RESULTS AND DISCUSSION

Figure 5 shows in the upper plot (a) the calculated bulk temperature and the measured surface temperature versus the heavy particle density n_i for a wire explosion with lowest (lower curve, $E_{max} = 350$ kJ/mol) and highest energy input (upper curve, $E_{max} = 2000$ kJ/mol). The boundary of the two-phase region (liquid-gas) has been approximately calculated using a critical-point exponent relation $\beta = 0.36$ [20]). Here a critical temperature of 12 500 K and a critical density of 2.29×10^{22} cm^{-3} was assumed as it was proposed in [11]. The measured ''surface'' temperature is always lower than the bulk temperature, shows inside the coexistence region a lower increase due to the latent heat needed for vaporization, and its increase with increasing expansion in the gaseous state is higher than that of the bulk temperature due to the lower specific heat. The different onset of melting can be explained with the dynamics of the process.

The averaged conductivity σ versus the averaged particle density n_i is shown in the lower plot (b) of Fig. 5. The measurements were carried out with different maximum energies and therefore also with different rates of energy dissipation, i.e., at different initial voltages on the capacitor. The resulting conductivity curves show good agreement; their deviations from an averaged curve are within the error bars. Further, the critical density n_c^L according to [11] is displayed. In addition, the experimental values from Hixson and Winkler [13], Zwikker [21], and Seydel, Fucke, and Wadle [22] are given as well as calculated conductivities using relations from Ziman ([23], $z = 6$) and from Likalter ([24]; $z = 3$,

$T = 12\,500$ K). Near the melting the conductivity agrees quite well with the Ziman theory [23] as it has been observed earlier for copper [9], too.

Around the critical density there exists a more or less extended domain [cf. Fig. 5(a)]—depending on the attained temperature (or pressure)—with a two-phase mixture (liquid-vapor) as long as it is passed below the critical temperature. Despite these different states, a smooth transition of the electrical conductivity was found during the expansion until finally—in the gaseous state—typical plasma values were obtained. The good agreement of the conductivity curves would mean that conductivity depends first of all on averaged heavy particle density and hence also on the electron density which decreases during expansion—also due to a decrease of the number of free electrons per atom. The dependence on the temperature in the range between 6000 and 13 000 K, however, seems to be very small. The corresponding phase-structure change (expanded fluid, fluid with bubbles, gas with droplets, dense plasma) obviously gives no reasons for drastic changes in the conductivity.

Due to the lack of knowledge about the number of free electrons during the expansion, the nonideality parameter Γ can only be estimated for some points, such as the melting point ($z = 6$, $\Gamma \approx 1000$), the critical point ($z \approx 3$, $\Gamma \approx 60$), and the maximal observed expansion ($z \approx 1$, $\Gamma \approx 2$).

[1] G.-F. Hohl, dissertation, Universität Marburg, 1992 (unpublished).

[2] B. Knuth, diplomarbeit, Universität Marburg, 1985 (unpublished).

[3] S. Jüngst, dissertation, Universität Marburg, 1985 (unpublished).

[4] R. Redmer, H. Reinholz, G. Röpke, R. Winter, F. Noll, and F. Hensel, J. Phys. Condens. Matter **4**, 1659 (1992).

[5] R. L. Shepherd, D. R. Kania, and L. A. Jones, Phys. Rev. Lett. **61**, 1278 (1988).

[6] J. F. Benage, Jr., W. R. Shanahan, E. G. Sherwood, L. A. Jones, and R. J. Trainor, Phys. Rev. E **49**, 4391 (1994).

[7] A. W. DeSilva and H. J. Kunze, Phys. Rev. E **49**, 4448 (1994).

[8] A. W. DeSilva, in *Proceedings of the International Conference on the Physics of Strongly Coupled Plasmas, Binz, Germany, 1995*, edited by W. D. Kraeft and M. Schlanges (World Scientific, Singapore, 1996).

[9] N. Ben-Yosef and A. G. Rubin, Phys. Rev. Lett. **23**, 289 (1969).

[10] L. Pauling, *The Nature of Chemical Bond* (Cornell University Press, Ithaca, 1960).

[11] H. Hess, Phys. Chem. Liq. **30**, 251 (1995).

[12] W. Köppendörfer, Institute of Plasma Physics, Garching, Germany, IPP-Berichte 1/2, 1961 (unpublished).

[13] R. S. Hixson and M. A. Winkler, Int. J. Thermophys. **11**, 709 (1990).

[14] E. Kaschnitz, G. Pottlacher, and L. Windholz, High Press. Res. **4**, 558 (1990).

[15] J. Emsley, *The Elements*, 2nd ed. (Clarendon, Oxford, 1992).

[16] E. Kaschnitz, dissertation, Technische Universität Graz, 1992 (unpublished).

[17] NARVA—former GDR lamp factory; wire normed by TGL Nr. 6994.

[18] M. v. Ardenne, *Tables of Applied Physics* (VEB Deutscher Verlag der Wissenschaften, Berlin, 1962), Vol. 1 (in German).

[19] H. Jäger, Habilitationsschrift, Universität Kiel, 1970 (unpublished).

[20] H. E. Stanley, *Introduction to Phase Transitions and Critical Phenomena* (Clarendon, Oxford, 1971); But cf. F. Hensel *et al.*, in *Localization and Metal-Insulator Transitions*, edited by H. Fritzsche and D. Adler (Plenum, New York, 1985).

[21] C. Zwikker, PHYSICA—Nederlandsch Tijdschrift voor Natuurkunde **5**, 249 (1925).

[22] U. Seydel, W. Fucke, and H. Wadle, *Die Bestimmung thermophysikalischer Daten flüssiger hochschmelzender Metalle mit schnellen Pulsaufheizexperimenten, Naturwissenschaftliche Studien, Metallphysik* (Verlag Dr. Peter Mannkopf, Düsseldorf, 1980).

[23] J. M. Ziman, *Prinzipien der Festkörperphysik* (Akademie-Verlag, Berlin, 1980).

[24] A. Likalter (private communication).